*Progress In Electromagnetics Research C, Vol. 65, 45–56, 2016*

# DOA and Polarization Estimation Algorithm Based on the Virtual Multiple Baseline Theory

**Guibao Wang[1, *], Mingxing Fu[1], Feng Zhao[1], and Xiang Liu[1, 2, 3]**

**Abstract**—An algorithm of solving phase ambiguity of multi-baseline direction finding system based on sparse uniform circular array is proposed in this paper. This sparse uniform circular array whose inter-element spacing is larger than half-wavelength distance suffers from cyclic phase ambiguities, which may cause estimation errors. In order to solve the above phase ambiguities, the corresponding virtual short baselines are acquired by transforming the array element phases that meet with the contraction relationship. The obtained short baselines are used to solve the phase ambiguities according to the virtual baseline and stagger baseline theory. Highly accurate estimates of direction of arrival are herein acquired. Furthermore, the direction of arrival and polarization parameter estimates are automatically matched with no additional processing. The array arrangement problem in high frequency scenario is solved. The estimation accuracy of angle of arrival is improved by means of the phase ambiguity resolution. Simulation results verify the effectiveness of this algorithm.

## 1. INTRODUCTION

Electromagnetic vector sensor array can obtain multi-dimensional information of electromagnetic signal, and it herein has the ability of spatial and polarization domain signal processing. The direction of arrival (abbreviated DOA) and polarization parameter estimations of multiple narrowband signals using electromagnetic vector sensor array techniques have a crucial role to play in many applications involving communication, radio astronomy, radar, sonar, seismic sensing, etc., and many valuable research results have been obtained [1–29]. Electromagnetic vector sensor can be divided into two categories: complete electromagnetic vector sensor (namely six-component electromagnetic vector sensor) and incomplete electromagnetic vector sensor (namely the antenna number of electromagnetic vector sensor is less than six). Particularly, the collocated loop and dipole pair has good performance because its antenna elements are not sensitive to the signal direction of arrival, which can decouple the polarization from direction of arrival [1–6].

A subspace algorithm to estimate direction of arrival and polarization by exploiting complete electromagnetic vector sensor was first proposed in [7–9]. Li and Compton [10] first applied estimations of signal parameters via rotational invariance techniques (abbreviated ESPRIT) to a vector-sensor array, and "vector-cross-product" DOA estimator was first applied to ESPRIT in [11, 12]. The uni-vector-sensor multiple signal classification (abbreviated MUSIC) algorithms were proposed in [13, 14]. Ref. [15] proposed an efficient two-dimensional direction finding method for improving estimation accuracy via aperture extension using the propagator method. The spread six-component electromagnetic vector-sensor direction-finding algorithms were proposed in [16, 17], which extended the spatial aperture at lower hardware cost. Ref. [18] proposed a novel disambiguation method using a MUSIC-like procedure to

*Received 17 April 2016, Accepted 7 June 2016, Scheduled 21 June 2016*

* Corresponding author: Guibao Wang (gbwangxd@126.com).

[1] School of Physics and Telecommunication Engineering, Shaanxi University of Technology, Hanzhong 723001, China. [2] School of Opto-electronic, Beijing Institute of Technology, Beijing 100081, China. [3] National Science and Technology Venture Capital Development Center, Beijing 100071, China.

identify the true direction cosine estimate from a set of cyclically related ambiguous candidate estimates. A novel closed-form ESPRIT-based algorithm using arbitrarily spaced electromagnetic vector-sensors was proposed in [19].

To ensure unambiguous angle estimations, it is required that the array inter-sensor spacing is less than half wavelength. However, the extended array aperture can offer enhanced array resolution but will cause the phase ambiguity of angle estimates. Therefore, resolving the phase ambiguity of array aperture extension is important [20–22], and the contribution of some work lies in that direction. Wang and co-authors proposed a DOA and polarization joint estimation method based on uniform concentric circular array [20], in which the phase differences between two array elements on inner circle were used to give rough but unambiguous estimates of DOA and as coarse references to disambiguate the cyclic phase ambiguities in phase differences between two array elements on outer ring circle. In [21], a two-dimensional DOA and polarization estimation algorithm for coherent sources using a linear vector-sensor array is presented. Yuan put forward the direction finding and polarization estimation method by using the spatially spread dipole/loop quads/quints in literature [22]. A 2-D direction finding algorithm with a sparse uniform array was introduced in [23], and the disambiguation of the resulting cyclic ambiguities was accomplished by the use of arrival angle information.

In this paper, we present a new phase ambiguity resolution approach based on the virtual multiple baseline theory [24–27]. The estimated phase differences are implemented by virtual array transformation when the phase differences of array elements satisfy certain conditions, and the ambiguous phase differences are herein resolved. The unambiguous but coarse phase differences are used to disambiguate the true phase differences of original array.

## 2. SIGNAL AND ARRAY MODELS

The receiving uniform circular array is composed of $M$ identical collocated loop and dipole pair, whose antenna elements are distributed over a circle with radius $R$. Supposing that the center of circle is located at the origin, the reference element of the array is a collocated loop and dipole, which is placed at origin, and the whole array elements are placed in the $x$-$y$ plane, as shown in Fig. 1.

The collocated loop and dipole pairs' steering vector of the $k$th ($1 \leq k \leq K$) unit-power electromagnetic source signal is $2 \times 1$ vector as follows:

$$\begin{bmatrix} e_{kz} \\ h_{kz} \end{bmatrix} = \begin{bmatrix} -\sin\theta_k \sin\gamma_k e^{j\eta_k} \\ \sin\theta_k \cos\gamma_k \end{bmatrix} \tag{1}$$

where $\theta_k \in [0, \pi/2]$ is the signal's elevation measured from the positive $z$-axis; $\gamma_k \in [0, \pi/2]$ symbolizes the auxiliary polarization angle; $\eta_k \in [-\pi, \pi]$ represents the polarization phase difference. $h_{kz}$ and $e_{kz}$ denote the $z$-axis magnetic and electric field received by loop and dipole at the origin of the coordinates.

$K$ ($K < M$) narrowband completely polarized electromagnetic plane wave source signals from far-field impinge upon an array, and the output of the uniform circular array at time $t$ can be written

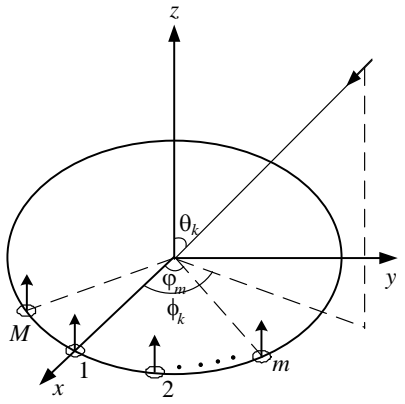


**Figure 1.** Uniform circular collocated loop and dipole array geometry.

compactly as

$$\mathbf{X}(t) = \begin{bmatrix} \mathbf{B}_1 \\ \mathbf{B}_2 \end{bmatrix} \mathbf{S}(t) + \mathbf{N}(t) = \mathbf{B}\mathbf{S}(t) + \mathbf{N}(t) \tag{2}$$

where $\mathbf{X}(t)$ is the received signal, $\mathbf{B}$ the $(2M+2) \times K$ array manifold matrix for the $K$ incident signals, $\mathbf{S}(t)$ the incident signal and $\mathbf{N}(t)$ the noise. $B_1$ and $B_2$ are respective the sub-array steering vectors of $M+1$ loops and $M+1$ dipoles, which can be represented as

$$\mathbf{B}_1 = [\sin\theta_1 \cos\gamma_1 \mathbf{q}(\theta_1, \phi_1), \ldots, \sin\theta_K \cos\gamma_K \mathbf{q}(\theta_K, \phi_K)] \tag{3}$$

$$\mathbf{B}_2 = \left[-\sin\theta_1 \sin\gamma_1 e^{j\eta_1} \mathbf{q}(\theta_1, \phi_1), \ldots, -\sin\theta_K \sin\gamma_K e^{j\eta_K} \mathbf{q}(\theta_K, \phi_K)\right] \tag{4}$$

where

$$\mathbf{q}(\theta_k, \phi_k) = \left[1, e^{j\varphi_{k,1}}, \ldots, e^{j\varphi_{k,m}}, e^{j\varphi_{k,M}}\right] \tag{5}$$

with the phase difference between the $m$th element and reference element of array $\varphi_{k,m}$ defined in Eq. (6).

$$\varphi_{k,m} = \frac{2\pi R}{\lambda_k} \sin\theta_k \cos(\phi_k - \varphi_m) \tag{6}$$

where $\varphi_m = 2\pi(m-1)/M$, $m = 1, \ldots, M$ determines the angular location of antenna $m$ on the circle, and $\phi_k \in [-\pi, \pi]$ denotes the signal's azimuth measured from the positive $x$-axis.

The true phase differences between the $M$ elements and reference element of array can be obtained:

$$\mathbf{\Phi}_k = [\varphi_{k,1}, \ldots, \varphi_{k,m}, \ldots, \varphi_{k,M}] = \frac{2\pi R}{\lambda_k} \mathbf{W}_1 \mathbf{\Gamma}_k \tag{7}$$

where $\mathbf{W}_1$ is the matrix whose elements are involved in the array element angular position information, so we call $\mathbf{W}_1$ as angular position information matrix. $\mathbf{\Gamma}_k$ is the vector whose elements are composed of the direction cosine information. $\mathbf{W}_1$ and $\mathbf{\Gamma}_k$ have the following form:

$$\mathbf{W}_1 = \begin{bmatrix} 0 & 1 \\ \sin\left(\frac{2\pi}{M}\right) & \cos\left(\frac{2\pi}{M}\right) \\ \vdots & \vdots \\ \sin\left[(M-1)\frac{2\pi}{M}\right] & \cos\left[(M-1)\frac{2\pi}{M}\right] \end{bmatrix}, \quad \mathbf{\Gamma}_k = \begin{bmatrix} \sin\theta_k \sin\phi_k \\ \sin\theta_k \cos\phi_k \end{bmatrix} \tag{8}$$

From formulas (3) and (4), the following relationship can be obtained:

$$\mathbf{B}_2 = \mathbf{B}_1 \mathbf{\Phi} \tag{9}$$

where

$$\mathbf{\Phi} = \begin{bmatrix} -\tan\gamma_1 e^{j\eta_1} & & \\ & \ddots & \\ & & -\tan\gamma_K e^{j\eta_K} \end{bmatrix} \tag{10}$$

## 3. DOA AND POLARIZATION ESTIMATION ALGORITHM

### 3.1. Polarization and Phase Difference Estimation Model

The covariance matrix $\mathbf{R}_x$ can be written as

$$\mathbf{R}_x = E\left[\mathbf{X}\mathbf{X}^H\right] = \mathbf{B}\mathbf{R}_s\mathbf{B}^H + \sigma^2\mathbf{I} \tag{11}$$

where $\mathbf{R}_s$ denotes the correlation matrix of incident signals and $\sigma^2$ the white noise power. Let $\mathbf{E}_s$ represent the $(2M+2) \times K$ matrix composing of the $K$ eigenvectors corresponding to $K$ largest eigenvalues of $\mathbf{R}_x$. According to the subspace theory, there exists $K \times K$ nonsingular matrix $\mathbf{T}$, and the signal subspace can be represented explicitly as [14]

$$\mathbf{E}_s = \mathbf{B}\mathbf{T} = \begin{bmatrix} \mathbf{B}_1 \\ \mathbf{B}_2 \end{bmatrix} \mathbf{T} \quad \mathbf{E}_1 = \mathbf{B}_1\mathbf{T} \quad \mathbf{E}_2 = \mathbf{B}_2\mathbf{T} = \mathbf{B}_1\mathbf{\Phi}\mathbf{T} \tag{12}$$

Since both $\mathbf{E}_1$ and $\mathbf{E}_2$ are column full-rank, there is a unique nonsingular matrix $\mathbf{\Omega}$ such that

$$\mathbf{E}_1\mathbf{\Omega} = \mathbf{E}_2 \Rightarrow \mathbf{\Omega} = \left(\mathbf{E}_1^H\mathbf{E}_1\right)^{-1}\mathbf{E}_1^H\mathbf{E}_2 \tag{13}$$

$$\mathbf{\Omega}\mathbf{T}^{-1} = \mathbf{T}^{-1}\mathbf{\Phi} \tag{14}$$

It can be seen from Equation (14) that the estimation of $\mathbf{\Phi}$, namely $\hat{\mathbf{\Phi}}$, consists of $K$ eigenvalues of matrix $\mathbf{\Omega}$, and the full-rank matrix $\mathbf{T}^{-1}$ is composed of $K$ eigenvectors of matrix $\mathbf{\Omega}$.

From matrix $\hat{\mathbf{\Phi}}$, the auxiliary polarization angle and polarization phase difference are obtained:

$$\hat{\gamma}_k = \tan^{-1}\left(\left|\hat{\mathbf{\Phi}}_{k,k}\right|\right) \quad \hat{\eta}_k = \arg\left(-\hat{\mathbf{\Phi}}_{k,k}\right) \tag{15}$$

The estimates of $\mathbf{B}$, $\mathbf{B}_1$ and $\mathbf{B}_2$ can be obtained by

$$\hat{\mathbf{B}}_1 = \mathbf{E}_1\hat{\mathbf{T}}^{-1} \quad \hat{\mathbf{B}}_2 = \mathbf{E}_2\hat{\mathbf{T}}^{-1} \quad \hat{\mathbf{B}} = \mathbf{E}_s\hat{\mathbf{T}}^{-1} \tag{16}$$

The estimate of spatial steering vector $\hat{\mathbf{q}}(\theta_k, \phi_k)$ is obtained from the normalized $\hat{\mathbf{B}}_1$:

$$\hat{\mathbf{q}}(\theta_k, \phi_k) = \frac{\hat{\mathbf{B}}_1(2:\ M+1, k)}{\hat{\mathbf{B}}_1(1, k)} \tag{17}$$

From formula (17), the estimated phase difference between the $M$ elements and reference element of array can be obtained:

$$\hat{\mathbf{\Phi}}_k = \arg\left[\hat{\mathbf{q}}(\theta_k, \phi_k)\right] = \left[\hat{\varphi}_{k,1}, \ldots, \hat{\varphi}_{k,m}, \ldots, \hat{\varphi}_{k,M}\right] \tag{18}$$

where $\hat{\varphi}_{k,m}$ is the estimated value of phase difference $\varphi_{k,m}$.

The sparse uniform circular array whose radius is larger than half maximum wavelength will suffer from phase ambiguities, that is to say, the estimated phase differences matrix $\hat{\mathbf{\Phi}}_k$ and true phase differences matrix $\mathbf{\Phi}_k$ meet the following relationship:

$$\mathbf{\Phi}_k = \hat{\mathbf{\Phi}}_k + 2\pi\mathbf{p}_k \tag{19}$$

where $\mathbf{p}_k = [p_{k1}, p_{k2}, \ldots, p_{kM}]$ is the phase ambiguity vector. In order to obtain the exact direction of arrival information, vector $\mathbf{p}_k$ should be acquired.

### 3.2. Virtual Transformation and Phase Ambiguity Resolution

The virtual element of the array can be obtained by executing virtual transformations on two true array-elements. The phase difference between the $k$th virtual element and reference element of array can be expressed as follows:

$$\begin{aligned}\hat{\varphi}_{k,n} + \hat{\varphi}_{k,m} &= \frac{2\pi R}{\lambda_k}\sin\theta_k\left[\cos(\phi_k - \varphi_n) + \cos(\phi_k - \varphi_m)\right] \\ &= \frac{2\pi\left\{2R\cos\left[\frac{\pi}{M}(m-n)\right]\right\}}{\lambda_k}\sin\theta_k\cos\left[\phi_k - \left(\frac{m+n}{2} - 1\right)\cdot\frac{2\pi}{M}\right]\end{aligned} \tag{20}$$

From Equations (6) and (20), the radius of the virtual circular array becomes $R^{(1)} = 2R\cos\left[\pi(m-n)/M\right]$ after one time virtual array transformation. The necessary condition for the operation of virtual array transformation is that $R^{(1)}$ is less than $R$.

According to the relationship of $R^{(1)}$ and $R$, it can be obtained:

$$0 < \cos\left[\pi(m-n)/M\right] < \frac{1}{2} \tag{21}$$

According to formula (21), the relationship of $m$ and $n$ can be obtained:

$$M/3 < m - n < M/2 \quad \text{or} \quad M/3 < n - m < M/2 \tag{22}$$

The relationship of phase difference matrix before and after $L$ times of virtual array transformation can be summarized as follows.

*3.2.1. The Case of Same Angular Position Information Matrix*

When $i = (m+n)/2$ is integer, after one virtual array transformation, the phase difference matrix between the virtual $M$-element and reference element of array can be expressed as:

$$\hat{\mathbf{\Phi}}_k^{(1)} = \left[\hat{\varphi}_{k,1}^{(1)}, \hat{\varphi}_{k,2}^{(1)}, \ldots, \hat{\varphi}_{k,M}^{(1)}\right] \tag{23}$$

where $\hat{\varphi}_{k,i}^{(1)}$ is the phase difference between the $i$th ($i = 1, \ldots, M$) virtual element and reference element of array, with

$$\hat{\varphi}_{k,i}^{(1)} = \hat{\varphi}_{k,n} + \hat{\varphi}_{k,m} = \frac{2\pi R^{(1)}}{\lambda_k} \sin\theta_k \cos\left[\phi_k - (i-1)\cdot\frac{2\pi}{M}\right] \tag{24}$$

From formula (24), there exists the following relationship:

$$\hat{\mathbf{\Phi}}_k^{(1)} = \mathbf{T}_k^{(1)} \hat{\mathbf{\Phi}}_k \tag{25}$$

where $\mathbf{T}_k^{(1)}$ is the first time virtual array transformation matrix whose elements come from Equation (24).

Since there exist phase ambiguities in $\hat{\mathbf{\Phi}}_k^{(1)}$, the virtual array transformation needs to be done, provided that the virtual circular radius is larger than incident signal half wavelength. Suppose that the virtual circular radius $R^{(L)}$ is less than incident signal half wavelength after implementing $L$ times virtual array transformations, that is to say, $R^{(L)} < \lambda_k/2$. According to formulas (6) and (20), the following expression is obtained:

$$R^{(L)} = R\left[2\cos\frac{\pi(m-n)}{M}\right]^L \tag{26}$$

Suppose that the phase difference matrix and virtual transformation matrix after $L$ times virtual transformations are labeled as $\hat{\mathbf{\Phi}}_k^{(L)}$ and $\mathbf{T}_k^{(L)}$, then the following relationship can be obtained:

$$\hat{\mathbf{\Phi}}_k^{(L)} = \mathbf{T}_k^{(L)} \hat{\mathbf{\Phi}}_k^{(L-1)} = \left(\mathbf{T}_k^{(1)}\right)^L \hat{\mathbf{\Phi}}_k \tag{27}$$

with $\hat{\mathbf{\Phi}}_k^{(L)} = \left[\hat{\varphi}_{k,1}^{(L)}, \hat{\varphi}_{k,2}^{(L)}, \ldots, \hat{\varphi}_{k,M}^{(L)}\right]^T$.

The matrices $\hat{\mathbf{\Phi}}_k^{(L)}$ and $R^{(L)}$ also have the following form:

$$\hat{\mathbf{\Phi}}_k^{(L)} = \frac{2\pi R^{(L)}}{\lambda_k} \mathbf{W}_1 \hat{\mathbf{\Gamma}}_k \tag{28}$$

where $\hat{\mathbf{\Gamma}}_k = \left[\sin\hat{\theta}_k \sin\hat{\phi}_k, \sin\hat{\theta}_k \cos\hat{\phi}_k\right]^T$ is the coarse and unambiguous estimation of direction cosine, and $\mathbf{W}_1$ is defined in Equation (8). Since $R^{(L)} < \lambda_k/2$, there does not exist phase ambiguity in $\hat{\mathbf{\Phi}}_k^{(L)}$, that is to say, the elements $\hat{\varphi}_{k,i}^{(L)}$ in $\hat{\mathbf{\Phi}}_k^{(L)}$ are in the range of $-\pi$ to $\pi$, with $1 \le i \le M$.

Based on the foregoing analysis, the following relationship can be obtained:

$$\hat{\mathbf{\Phi}}_k^{(L)} = \mathbf{T}_k^{(L)} \hat{\mathbf{\Phi}}_k^{(L-1)} = \left(\mathbf{T}_k^{(1)}\right)^L \hat{\mathbf{\Phi}}_k = \frac{2\pi R^{(L)}}{\lambda_k} \mathbf{W}_1 \hat{\mathbf{\Gamma}}_k \tag{29}$$

The angular position information matrices of virtual and true circular arrays are the same, but the radii of the two arrays are different.

*3.2.2. The Case of Different Angular Position Information Matrix*

When $i = (m+n)/2$ is non-integer, let $d' = (m+n+1)/2$, and $d'$ is the sequence number of the virtual array. After one time virtual array transformation, the phase difference matrix between the virtual $M$-element and reference element of array can be represented as:

$$\hat{\mathbf{\Phi}}_k^{(1)} = \left[\hat{\varphi}_{k,1}^{(1)}, \hat{\varphi}_{k,2}^{(1)}, \ldots, \hat{\varphi}_{k,M}^{(1)}\right] \tag{30}$$

where $\hat{\varphi}_{k,d'}^{(1)}$ is the phase difference between the $d'$th $(d = 1, \ldots, M)$ virtual element and reference element of array, with

$$\hat{\varphi}_{k,d'}^{(1)} = \hat{\varphi}_{k,n} + \hat{\varphi}_{k,m} = \frac{2\pi R^{(1)}}{\lambda_k} \sin\theta_k \cos\left[\phi_k - \left(d' - \frac{1}{2}\right) \cdot \frac{2\pi}{M}\right] \tag{31}$$

From formula (31), there exists the following relationship:

$$\hat{\mathbf{\Phi}}_k^{(1)} = \mathbf{T}_{k1} \hat{\mathbf{\Phi}}_k \tag{32}$$

where $\mathbf{T}_{k1}$ is the first time virtual array transformation matrix whose elements are derived from Equation (31), and $\hat{\mathbf{\Phi}}_k^{(1)}$ is the phase difference matrix after the first time virtual array transformation.

The relation of $\hat{\mathbf{\Phi}}_k^{(1)}$ and $R^{(1)}$ can also be represented in matrix notation as follows:

$$\hat{\mathbf{\Phi}}_k^{(1)} = \frac{2\pi R^{(1)}}{\lambda_k} \mathbf{W}_2 \hat{\mathbf{\Gamma}}_k \tag{33}$$

where $\mathbf{W}_2$ is the matrix whose elements denote the angular position information, i.e.,

$$\mathbf{W}_2 = \begin{bmatrix} \sin\left(\frac{\pi}{M}\right) & \cos\left(\frac{\pi}{M}\right) \\ \sin\left(\frac{3\pi}{M}\right) & \cos\left(\frac{3\pi}{M}\right) \\ \vdots & \vdots \\ \sin\left[(2M-1)\frac{\pi}{M}\right] & \cos\left[(2M-1)\frac{\pi}{M}\right] \end{bmatrix} \tag{34}$$

From formulas (8) and (34), we can see that the matrix $\mathbf{W}_1$ is different from $\mathbf{W}_2$.

After two times of virtual array transformations, the phase differences can be expressed as follows:

$$\hat{\varphi}_{k,d''}^{(2)} = \hat{\varphi}_{k,n'}^{(1)} + \hat{\varphi}_{k,m'}^{(1)} = \frac{2\pi R^{(2)}}{\lambda_k} \sin\theta_k \cos\left[\phi_k - \left(d'' - 1\right) \cdot \frac{2\pi}{M}\right] \tag{35}$$

where $m'$ and $n'$ are the sequence numbers after one virtual transformation. Since $i' = (m' + n')/2$ is non-integer, $d'' = (m' + n' - 1)/2$ is integer. Furthermore, the phase differences $\hat{\varphi}_{k,d''}^{(2)}$ in Eq. (35) have the same form as $\hat{\varphi}_{k,i}^{(1)}$ in Eq. (24).

Equation (35) can be indicated with the following matrix form:

$$\hat{\mathbf{\Phi}}_k^{(2)} = \frac{2\pi R^{(2)}}{\lambda_k} \mathbf{W}_1 \mathbf{\Gamma}_k \tag{36}$$

Formula (35) can also be represented by the following matrix form

$$\hat{\mathbf{\Phi}}_k^{(2)} = \mathbf{T}_{k2} \hat{\mathbf{\Phi}}_k^{(1)} = \mathbf{T}_{k2} \mathbf{T}_{k1} \hat{\mathbf{\Phi}}_k \tag{37}$$

where $\mathbf{T}_{k2}$ and $\hat{\mathbf{\Phi}}_k^{(2)}$ are the virtual array transformation matrix and phase difference matrix after two times of virtual array transformation, which are determined by formula (35). Based on the above-mentioned analysis, it can be shown that the virtual angular position information matrix is the same as the true angular position information matrix after two times of virtual transformations. Meanwhile, the radii of the virtual circular array and initial circular arrays are different.

The true phase difference matrix can be obtained if $R^{(1)}$ or $R^{(2)}$ is less than incident signal half wavelength. Otherwise, $\hat{\mathbf{\Phi}}_k^{(1)}$ or $\hat{\mathbf{\Phi}}_k^{(2)}$ has phase ambiguities, and the virtual transformation herein needs to be continued until the virtual circular radius is less than incident signal half wavelength. Supposing that $R^{(L)}$ defined in formula (26) is less than half wavelength of the incident signal after conducting $L$ times virtual transformations, the corresponding phase difference matrix is labeled as $\hat{\mathbf{\Phi}}_k^{(L)}$, where $L$ is the minimal positive integer that meets Equation (26). To obtain the phase difference matrix, two cases of virtual transformation are discussed. In the two possible conditions,

1) The number of virtual array transformation times $L$ is odd, and the relation between $\hat{\mathbf{\Phi}}_k^{(L)}$ and $\hat{\mathbf{\Phi}}_k$ are summarized as follows:

$$\hat{\mathbf{\Phi}}_k^{(L)} = \frac{2\pi R_k^{(L)}}{\lambda_k}\mathbf{W}_2\hat{\mathbf{\Gamma}}_k = \mathbf{T}_{k1}\left(\mathbf{T}_{k2}\mathbf{T}_{k1}\right)^{\frac{L-1}{2}}\hat{\mathbf{\Phi}}_k \tag{38}$$

where $L$ is the minimal positive even number that meets $R^{(L)} < \lambda_k/2$, and $R^{(L)}$ has the form in Equation (26). $\hat{\mathbf{\Phi}}_k$ is the original phase difference matrix.

2) The number of virtual array transformation times $L$ is even, and the relation between $\hat{\mathbf{\Phi}}_k^{(L)}$ and $\hat{\mathbf{\Phi}}_k$ are summarized as follows:

$$\hat{\mathbf{\Phi}}_k^{(L)} = \frac{2\pi R_k^{(L)}}{\lambda_k}\mathbf{W}_1\hat{\mathbf{\Gamma}}_k = \left(\mathbf{T}_{k2}\mathbf{T}_{k1}\right)^{\frac{L}{2}}\hat{\mathbf{\Phi}}_k \tag{39}$$

### 3.3. Phase Ambiguity Resolution in Direction Finding

According to Equations (29), (38) and (39), we get the coarse and unambiguous estimate $\hat{\mathbf{\Gamma}}_k$:

$$\hat{\mathbf{\Gamma}}_k = \mathbf{W}^{\#}\hat{\mathbf{\Phi}}_k^{(L)} = \mathbf{W}^{\#}\mathbf{T}_k^{(L)}\hat{\mathbf{\Phi}} \tag{40}$$

where $\mathbf{W}^{\#} = \left(\mathbf{W}^H\mathbf{W}\right)^{-1}\mathbf{W}^H$ is a pseudo-inverse matrix of $\mathbf{W}$, with

$$\begin{cases} \mathbf{W} = \dfrac{2\pi R_k^{(L)}}{\lambda_k}\mathbf{W}_1, \quad \mathbf{T}_k^{(L)} = \left(\mathbf{T}_k\right)^L & \text{when } \dfrac{m+n}{2} \text{ and } L \text{ are intergers} \\ \mathbf{W} = \dfrac{2\pi R_k^{(L)}}{\lambda_k}\mathbf{W}_2, \quad \mathbf{T}_k^{(L)} = \mathbf{T}_{k1}\left(\mathbf{T}_{k2}\mathbf{T}_{k1}\right)^{\frac{L-1}{2}} & \text{when } \dfrac{m+n}{2} \text{ is non-interger, } L \text{ is odd number} \\ \mathbf{W} = \dfrac{2\pi R_k^{(L)}}{\lambda_k}\mathbf{W}_1, \quad \mathbf{T}_k^{(L)} = \left(\mathbf{T}_{k2}\mathbf{T}_{k1}\right)^{\frac{L}{2}} & \text{when } \dfrac{m+n}{2} \text{ is non-interger, } L \text{ is even number} \end{cases}.$$

By substitution of Eq. (40) into Eq. (41), the coarse but unambiguous estimations of the true phase difference matrix $\bar{\mathbf{\Phi}}$ are obtained as follows:

$$\bar{\mathbf{\Phi}}_k = \frac{2\pi R}{\lambda_k}\mathbf{W}_1\hat{\mathbf{\Gamma}}_k \tag{41}$$

From formulas (19) and (41), a method is developed for solving the phase cycle number ambiguity vector $\mathbf{p}_{k,\,opt}$, and this problem is formulated as the optimization procedure:

$$\mathbf{p}_{k,\,opt} = \arg\min_{\mathbf{p}_k}\left|\bar{\mathbf{\Phi}}_k - \left(\hat{\mathbf{\Phi}}_k + 2\pi\mathbf{p}_k\right)\right| \tag{42}$$

From Eq. (42), the estimates of true phase difference matrix $\tilde{\mathbf{\Phi}}$ can be obtained as:

$$\tilde{\mathbf{\Phi}}_k = \hat{\mathbf{\Phi}}_k + 2\pi\mathbf{p}_{k,\,opt} \tag{43}$$

Here $\tilde{\mathbf{\Phi}}$ is the high-precision estimation.
According to Equations (7) and (43), it is shown that

$$\tilde{\mathbf{\Phi}}_k = \mathbf{E}_k\tilde{\mathbf{\Gamma}}_k \tag{44}$$

where

$$\mathbf{E}_k = \frac{2\pi R}{\lambda_k}\mathbf{W}_1 \quad \tilde{\mathbf{\Gamma}}_k = \begin{bmatrix} \tilde{\Gamma}_{k1} \\ \tilde{\Gamma}_{k2} \end{bmatrix} = \begin{bmatrix} \sin\tilde{\theta}_k\sin\tilde{\phi}_k \\ \sin\tilde{\theta}_k\cos\tilde{\phi}_k \end{bmatrix} \tag{45}$$

The accurate direction cosine estimates are obtained by employing the least square norm:

$$\tilde{\mathbf{\Gamma}}_k = \begin{bmatrix} \tilde{\Gamma}_{k1} \\ \tilde{\Gamma}_{k2} \end{bmatrix} = \begin{bmatrix} \sin\tilde{\theta}_k\sin\tilde{\phi}_k \\ \sin\tilde{\theta}_k\cos\tilde{\phi}_k \end{bmatrix} = \mathbf{E}_k^{\#}\tilde{\mathbf{\Phi}}_k \tag{46}$$

where $\mathbf{E}_k^{\#} = \left(\mathbf{E}_k^H \mathbf{E}_k\right)^{-1} \mathbf{E}_k^H$ is a pseudo-inverse matrix of $\mathbf{E}_k$.

According to formula (46), the accurate estimates of direction of arrival are obtained:

$$\begin{cases} \tilde{\theta}_k = \arcsin\sqrt{\tilde{\Gamma}_{k1}^2 + \tilde{\Gamma}_{k2}^2} \\ \begin{cases} \tilde{\phi}_k = \arctan\left(\dfrac{\tilde{\Gamma}_{k1}}{\tilde{\Gamma}_{k2}}\right), & \tilde{\Gamma}_{k2} \geq 0 \\ \tilde{\phi}_k = \pi + \arctan\left(\dfrac{\tilde{\Gamma}_{k1}}{\tilde{\Gamma}_{k2}}\right), & \tilde{\Gamma}_{k2} < 0 \end{cases} \end{cases} \tag{47}$$

Our proposed virtual transformation method for estimating the direction of arrival and polarization parameters can herein be summarized as follows.

1) Measure the phase differences $\hat{\mathbf{\Phi}}_k$ between the array element and the origin of coordinate, and $\hat{\mathbf{\Phi}}_k$ is ambiguous.
2) The matrix $\hat{\mathbf{\Phi}}_k^{(L)}$ whose phase difference is unambiguous, and the coarse estimates of direction cosine $\hat{\mathbf{\Gamma}}_k$ are obtained according to the virtual transformation Equation (40).
3) The number of phase cycle ambiguities of the true phase difference matrix is acquired according to formula (42), thus the true phase difference matrix $\tilde{\mathbf{\Phi}}_k$ is achieved, and the DOA estimates are herein obtained.

## 4. SIMULATION RESULTS

In this section, the direction of arrival and polarization parameter estimation experiments are carried out to verify the effectiveness of the proposed method. Incident signal source with parameters $(\theta_1, \phi_1, \gamma_1, \eta_1) = (28°, 45°, 65°, 78°)$ and $(\theta_2, \phi_2, \gamma_2, \eta_2) = (72°, 85°, 35°, 120°)$ impinge upon a sparse 7-element uniform circular array with a radius of $R = 3.5\lambda$, as shown in Fig. 1. 200 independent Monte Carlo trials and 512 temporal snapshots are used in these simulations. The simulation results are shown in Figs. 2–8.

In the first experiment, we consider the scatter diagrams of elevation and azimuth. The signal-to-noise ratio (abbreviated SNR) is set to 15 dB, and the sets of values of the DOA variables have been represented in Figs. 2 and 3.

The true values of direction of arrival are $(\theta_1, \phi_1) = (28°, 45°)$ and $(\theta_2, \phi_2) = (72°, 85°)$. From Fig. 3, we can see that the perturbation of the estimated values using virtual array is small, and the estimated values of direction of arrival, namely $\hat{\theta}_1$ and $\hat{\phi}_1$, are respectively the numerical ranges

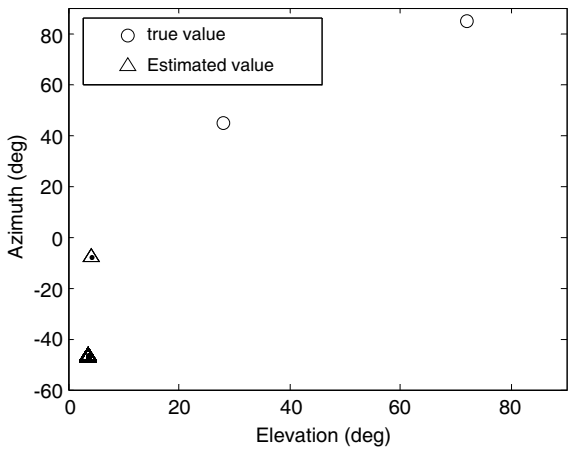


**Figure 2.** Scatter diagram using original array.

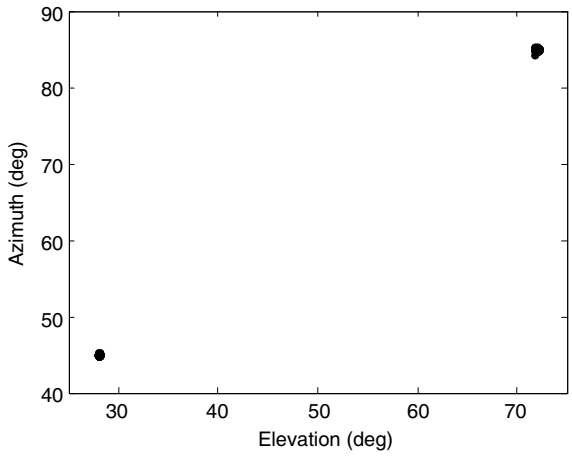


**Figure 3.** Scatter diagram using virtual array.

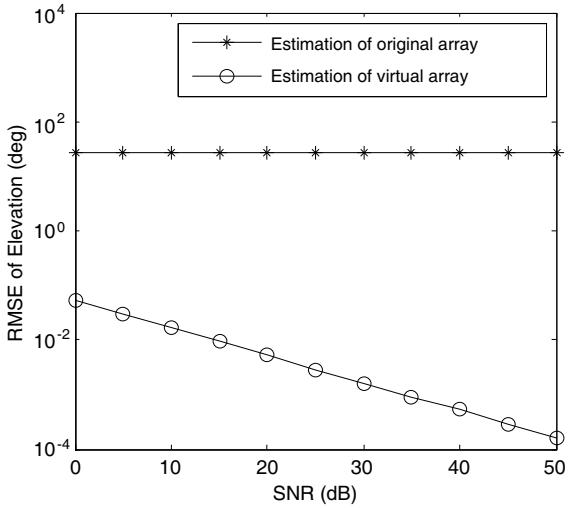


**Figure 4.** RMSE of elevation versus SNR.

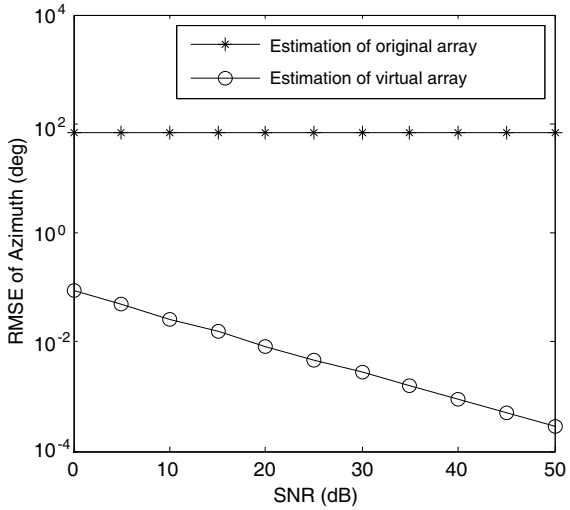


**Figure 5.** RMSE of azimuth versus SNR.

$\hat{\theta}_1 \in (27.9°, 28.1°)$ and $\hat{\phi}_1 \in (44.85°, 45.15°)$. Similarly, the estimated values of $\hat{\theta}_2$ and $\hat{\phi}_2$ are respectively the numerical ranges $\theta_2 \in (71.8°, 72.2°)$ and $\phi_2 \in (84.8°, 85.2°)$. On the contrary, using the original array the estimated points of azimuth are wrongly distributed in the ranges of $\phi_1 \in (-7.75°, -7.65°)$ and $\phi_2 \in (-46.7°, -47.3°)$, and the estimated points of elevation are wrongly distributed in the ranges of $\theta_1 \in (4.16°, 4.18°)$ and $\theta_2 \in (3.48°, 3.52°)$, as shown in Fig. 2.

In the second experiment, we consider the performance of the estimations of DOA and polarization. Without loss of generality, we discuss only the signal one. The root mean square error (abbreviated RMSE) of the DOA and polarization variables are represented in Figs. 4–7, and the SNR ranges in Figs. 4-7 are from 0 dB to 50 dB.

Figure 4 shows that the RMSE of elevation using original array is 27.55°. The RMSE of elevation using the virtual array is 0.053° at SNR = 0. Moreover, the RMSE of elevation decreases evidently as the SNR increases. Similarly, the RMSEs of azimuth using the original and virtual array are indicated in Fig. 5, and the RMSE of azimuth using the original array is 69°. In the SNR range (namely, at or above 0 dB), the RMSE of azimuth is degraded significantly using the virtual array, and the RMSE of azimuth is 0.09° at SNR = 0. The reason that the estimation using original array has larger deviation is as follows: the existence of phase ambiguity makes the estimates have larger deviation, which cannot be overcome even if improving the SNR. The virtual transform processing can effectively solve the problem of phase ambiguity. Hence the precise estimates of DOA can be obtained.

Figures 6–7 respectively plot the estimation RMSE of polarization phase difference and auxiliary polarization angle, respectively estimated using the virtual array and original array, at various SNR levels. The two estimated results are nearly the same because the sparse embattle of uniform circular array has little influence on polarization phase difference and auxiliary polarization angle.

In Figs. 4 and 5, the RMSE using the original array is plotted as the horizontal line, because the phase ambiguities exist, and then the estimates have larger deviations. For example, the average estimated value of elevation using the original array is 28° and the corresponding average estimated values of azimuth is 69°. The disturbances of all the estimated values appear around the average estimated values. The disturbances grow smaller and smaller with the increase of SNR, which is too small relative to the average deviation to be shown in Figs. 4 and 5.

In order to further illustrate the above issues, in the following experiment, we consider the performance of standard deviation estimations of direction of arrival. The SNR ranges from 0 dB to 50 dB, and the standard deviation of elevation is shown in Fig. 8. From Fig. 8 it is shown that the estimation performances of elevation using the original and virtual array both beome better and better with the increase of SNR. However, Fig. 8 shows that the estimated value gets closer and closer to a certain value. From Figs. 2 and 3, we can see that this certain value described above is 4.17°. By contrast, the value of the actual elevation value is 28°. The simulation and discussion for the azimuth

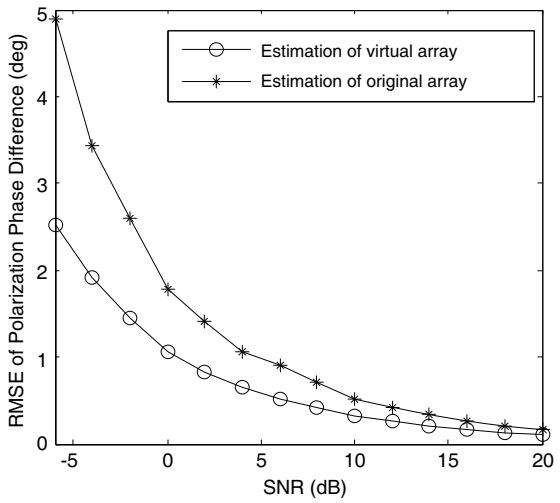


**Figure 6.** RMSE of polarization phase difference versus SNR.

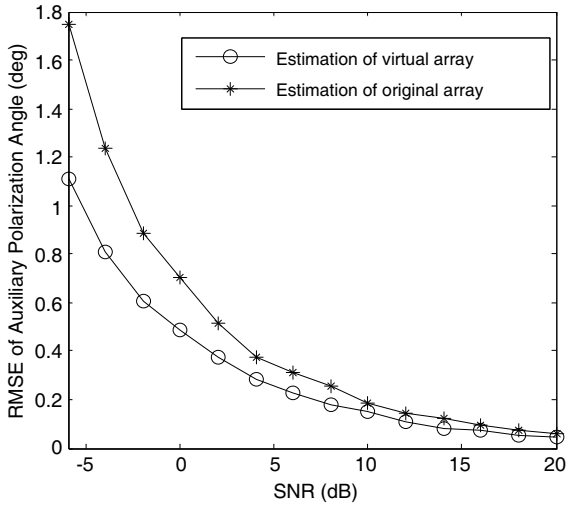


**Figure 7.** RMSE of auxiliary polarization angle versus SNR.

are similar to that of the elevation.

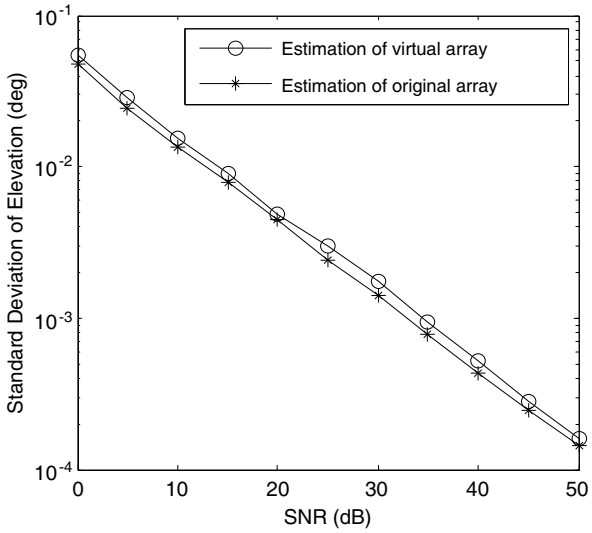


**Figure 8.** Standard deviation of elevation versus SNR.

## 5. CONCLUSION

A new algorithm for estimating DOA and polarization using sparse uniform circular collocated loop and dipole array is proposed in this paper. The process of phase ambiguity resolution of DOA estimation can be summarized as follows. In the first step, the array elements whose phases satisfy the contraction transformation condition are acquired, and the phase differences between these array elements and the origin of coordinates are herein obtained. In the second step, the virtual transformations are done to the obtained phase differences, and the short baselines are herein obtained. These short baselines are used to solve the phase ambiguity of long baseline. Finally, according to the position matrix before and after the virtual transformation, the high-precision DOA estimations are obtained using the least square method. The new method not only solves the phase ambiguity of DOA estimation of sparse array, but also obtains a high-precision DOA estimation performance.

## ACKNOWLEDGMENT

This work was supported by the National Natural Science Foundation of China (61475094, 61201295) and also supported by the projects program of Shaanxi University of Technology Academician Workstation (fckt201504). The authors would like to thank the anonymous reviewers and the associated editor for their valuable comments and suggestions that improved the clarity of this manuscript. We also thank L. M. Wang very much for all the help she gave us when we wrote this manuscript.

## REFERENCES

1. Yuan, X., K. T. Wong, Z. Xu, and K. Agrawal, "Various compositions to form a triad of collocated dipoles/loops, for direction finding and polarization estimation," *IEEE Sens. J.*, Vol. 12, No. 6, 1763–1771, 2012.
2. Wang, G., "A joint parameter estimation method with conical conformal CLD pair array," *Progress In Electromagnetics Research C*, Vol. 57, 99–107, 2015.
3. Li, Y. and J. Q. Zhang, "An enumerative nonlinear programming approach to direction finding with a general spatially spread electromagnetic vector sensor array," *IEEE Trans. Signal Process.*, Vol. 93, 856–865, 2013.
4. Yuan, X., K. T. Wong, and K. Agrawal, "Polarization estimation with a dipole-dipole pair, a dipole-loop pair, or a loop-loop pair of various orientations," *IEEE Trans. Antenn. Propag.*, Vol. 60, No. 5, 2442–2452, 2012.
5. Luo, F. and X. Yuan, "Enhanced 'vector-cross-product' direction-finding using a constrained sparse triangular-array," *EURASIP J. Adv. Signal Process.*, Vol. 2012, No. 115, 1–11, 2012.
6. Wang, L. M., Z. H. Chen, and G. B. Wang, "Direction finding and positioning algorithm with COLD-ULA based on quaternion theory," *Journal of Communications*, Vol. 9, No. 10, 778–784, 2014.
7. Nehorai, A. and E. Paldi, "Vector-sensor array processing for electromagnetic source localization," *25th Asilomar Conf. Signals, Syst., Comput.*, 566–572, Pacific Grove, CA, 1991.
8. Nehorai, A. and E. Paldi, "Vector sensor array processing for electromagnetic source localization," *IEEE Trans. Signal Process.*, Vol. 42, No. 2, 376–398, 1994.
9. Li, J., "Direction and polarization estimation using arrays with small loops and short dipoles," *IEEE Trans. Antenn. Propag.*, Vol. 41, No. 3, 379–387, 1993.
10. Li, J. and R. T. Compton, "Two-dimensional angle and polarization estimation using the ESPRIT algorithm," *IEEE Trans. Antenn. Propag.*, Vol. 40, No. 5, 550–555, 1992.
11. Wong, K. T. and M. D. Zoltowski, "Polarization diversity and extended aperture spatial diversity to mitigate fading-channel effects with a sparse array of electric dipoles or magnetic loops," *IEEE Int. Veh. Technol. Conf.*, 1163–1167, 1997.
12. Wong, K. T. and M. D. Zoltowski, "High accuracy 2D angle estimation with extended aperture vector sensor arrays," *Proc. IEEE. Int. Conf. Acoust., Speech, Signal Processing*, Vol. 5, 2789–2792, 1996.
13. Wang, L. M., L. Yang, G. B. Wang, and Z. H. Chen, "Uni-vector-sensor dimensionality reduction MUSIC algorithm for DOA and polarization estimation," *Math. Probl. Eng.*, Vol. 2014, 1–9, 2014.
14. Wong, K. T. and M. D. Zoltowski, "Uni-vector-sensor ESPRIT for multisource azimuth, elevation, and polarization estimation," *IEEE Trans. Antenn. Propag.*, Vol. 45, No. 10, 1467–1474, 1997.
15. He, J. and Z. Liu, "Extended aperture 2-D direction finding with a two-parallel-shape-array using propagator method," *IEEE Antenn. Wirel. Pr.*, Vol. 8, 323–327, 2009.
16. Wong, K. T. and X. Yuan, "Vector cross-product direction-finding' with an electromagnetic vector-sensor of six orthogonally oriented but spatially non-collocating dipoles/loops," *IEEE Trans. Signal Process.*, Vol. 59, No. 1, 160–171, 2011.
17. Song, Y., X. Yuan, and K. T. Wong, "Corrections to 'vector cross-product direction-finding' with an electromagnetic vector-sensor of six orthogonally oriented but spatially non-collocating dipoles/loops," *IEEE Trans. Signal Process.*, Vol. 62, No. 4, 1028–1030, 2014.

18. Zoltowski, M. D. and K. T. Wong, "Closed-form eigenstructure-based direction finding using arbitrary but identical subarrays on a sparse uniform rectangular array grid," *IEEE Trans. Signal Process.*, Vol. 48, No. 8, 2205–2210, 2000.
19. Wong, K. T. and M. D. Zoltowski, "Closed-form direction-finding with arbitrarily spaced electromagnetic vector-sensors at unknown locations," *IEEE Trans. Antenn. Propag.*, Vol. 48, No. 5, 671–681, 2000.
20. Wang, L. M., G. B. Wang, and Z. H. Chen, "Joint DOA-polarization estimation based on uniform concentric circular array," *Journal of Electromagnetic Waves and Applications*, Vol. 27, No. 13, 1702–1714, 2013.
21. Liu, J., Z. Liu, and Q. Liu, "Direction and polarization estimation for coherent sources using vector sensors," *Journal of Systems Engineering and Electronics*, Vol. 24, No. 4, 600–605, 2013.
22. Yuan, X., "Spatially spread dipole/loop quads/quints: For direction finding and polarization estimation," *IEEE Antennas Wireless Propag. Lett.*, Vol. 12, 1081–1084, 2013.
23. Zoltowski, M. D. and K. T. Wong, "ESPRIT-based 2D direction finding with a sparse array of electromagnetic vector-sensors," *IEEE Trans. Signal Process.*, Vol. 48, No. 8, 2195–2204, 2000.
24. Gavish, M. and A. J. Weiss, "Array geometry for ambiguity resolution in direction finding," *IEEE Trans. Antenn. Propag.*, Vol. 44, No. 6, 889–895, 1996.
25. Zhou, Y. Q. and F. K. Huang, "Solving ambiguity problem of digitized multi-baseline interferometer under noisy circumstance," *Journal of China Institute of Communications*, Vol. 34, No. 8, 16–21, 2005.
26. Wang, L. M., J. P. Lin, G. B. Wang, and Z. H. Chen, "A direction finding technique using millimeter-wave interferometer," *J. Infrared Millim. W.*, Vol. 34, No. 2, 140–144, 2015.
27. Wu, Y. W., S. Rhodes, and E. H. Satorius, "Direction of arrival estimation via extended phase interferometry," *IEEE Trans. Aero. Elec. Sys.*, Vol. 31, No. 1, 375–381, 1995.
28. Wang, G. B., "Direction of arrival and polarization estimation with a polarized circular array," *Journal of Beijing University of Posts and Telecommunications*, Vol. 39, No. 2, 72–75, 2016.
29. Lominé, J., C. Morlaas, C. Imbert, and H. Aubert, "Dual-band vector sensor for direction of arrival estimation of incoming electromagnetic waves," *IEEE Trans. Antenn. Propag.*, Vol. 63, No. 8, 3662–3671, 2015.